Available online at www.sciencedirect.com
ScienceDirect
Talanta 74 (2007) 212–222
Talanta
www.elsevier.com/locate/talanta

Preparation and characterization of PtAu hybrid film modified electrodes and their use in simultaneous determination of dopamine, ascorbic acid and uric acid

Soundappan Thiagarajan, Shen-Ming Chen *

Electroanalysis and Bioelectrochemistry Lab, Department of Chemical Engineering and Biotechnology, National Taipei University of Technology, No.1, Section 3, Chung-Hsiao East Road, Taipei 106, Taiwan, ROC

Received 26 February 2007; received in revised form 25 May 2007; accepted 29 May 2007
Available online 3 June 2007

Abstract

A novel biosensor was fabricated by electrochemical deposition of platinum and gold nanoparticles (nanoAu) with L-Cysteine on glassy carbon electrode. It was found that the nanoAu particle size distribution range was (50–80 nm), and the platinum particle size range was (200–300 nm). The hybrid film could be produced on gold and transparent indium tin oxide electrodes for different kind of studies such as electrochemical quartz crystal microbalance (EQCM), scanning electron microscopy (SEM), atomic force microscopy (AFM) and X-ray diffraction (XRD) and electrochemical studies. The PtAu hybrid film was applied to the electro catalytic oxidation of dopamine (DA), ascorbic acid (AA) and uric acid (UA) at pH 4.0 using cyclic voltammetry (CV) and differential pulse voltammetry (DPV) techniques. The modified electrode was quite effective not only to detect DA, AA and UA individually but also in simultaneous determination of these species in a mixture. The overlapping anodic peaks of DA, AA and UA were resolved into three well-defined voltammetric peaks in CV and DPV. The catalytic peak currents obtained from CV and DPV increased linearly with concentration. The relative standard deviation (% R.S.D., $n = 10$) for AA, DA and UA were less than 2.0% and DA, AA and UA can be determined in the ranges of 0.103–1.65, 0.024–0.384 and 0.021–0.336 mM, respectively. In addition, the modified electrode also shows good sensitivity, and stability. Satisfactory results were achieved for the determination of DA, AA and UA in dopamine injection solution, vitamin C tablets and human urine samples.

Keywords: PtAu hybrid film; L-Cysteine; Dopamine; Ascorbic acid; Uric acid; Simultaneous determination

1. Introduction

Electroanalytical methods have been used during the past three decades to investigate the role of neurotransmitters in the brain due to their electroactive nature [1]. In that the chemically modified electrodes have been widely used as sensitive and favorable analytical methods [2,3]. Simultaneous detection of dopamine (DA), ascorbic acid (AA) and uric acid (UA) is a problem of critical importance not only in the field of biomedical chemistry and neurochemistry but also for diagnostic and pathological research. DA which was discovered to be an important neurotransmitter in mammalian central nervous system found in high amounts (50 nmol/g) in a region of the brain known as the "caudate nucleus". The very low concentration of DA in the "extracellular fluid" of the caudate nucleus provides a large challenge for detection of DA. It was also found that patients with Parkinson's disease show an almost complete depletion of DA in this region. So, DA is currently the subject of intense research focus to neuroscientists and chemists and it is essential to develop rapid and simple methods for the determination of DA. The common instrumental techniques like high performance liquid chromatography (HPLC) have been widely used for the determination of DA [4]. However, such methods of detection are often complicated and very expensive. The electrochemical oxidation of DA has been studied and the results show that the electrochemical oxidation is a two-electron irreversible process with transfer of two protons [5]. The various inorganic and organic materials [6], Langmuir-Blodgett (LB) film [7], microfluidicsystem [8], biomemetic approach [9], sol–gel material based electrodes [10], enzymeless biosensor [11], bien-

* Corresponding author. Tel.: +886 2 27017147; fax: +886 2 27025238.
E-mail address: smchen78@ms15.hinet.net (S.-M. Chen).

0039-9140/$ – see front matter © 2007 Elsevier B.V. All rights reserved.
doi:10.1016/j.talanta.2007.05.049

zymatic system [12], enzyme amplification system [13] and voltammetric electrodes [14] have been reported for oxidation of DA.

AA (vitamin C) present in both animal and plant kingdoms, is a vital component in human diet. Among animal organs, the liver, leukocytes and anterior pituitary lobe show the highest concentrations of AA. It is present in mammalian brain along with several neurotransmitter amines. AA has been used for the prevention and treatment of common cold, mental illness, infertility, cancer and AIDS. It is widely used in foods and drinks as an antioxidant. The Prussian blue [15], ruthenium (III) diphenyldithiocarbamate [16], polypyrrole/ferrocyanide [17], polyaniline [18], polyglycine [19], poly(*N*,*N*-dimethylaniline) [20], poly(*p*-aminobenzene sulfonic acid) [21] have been used to fabricate modified electrode which can enhance the electron transfer rate and reduce the overpotential for the oxidation of AA.

On the other hand, UA is the primary end product of purine metabolism. Abnormal levels of UA are symptoms of several diseases such as gout, hyperuricemia and Lesch-Nyan disease. In general, electroactive UA can be irreversibly oxidized in aqueous solution and the major product is allantoin [22]. The various methods such as enzyme-based techniques [23], chemically modified electrodes [24,25] and fluorescent sol–gel biosensors [26] were developed to solve the UA detection problem. The nafion-modified electrodes were especially interesting for the determination of DA in the presence of AA [27,28]. Silver and copper dispersed composite electrodes prepared by sol–gel method, carbon paste electrode modified with titanium phosphated silica gel used for determination of AA and DA [29,30]. However, these kinds of modified electrodes suffer from slow response due to low diffusion coefficients of analytes in the films. It is known that at a bare electrode the oxidation peaks of DA and AA are at nearly same potential, which is resulted in the overlapped voltammetric responses making their discrimination highly difficult [5]. To determine DA in the presence of a large excess of AA or to perform their simultaneous determination, some electroanalytical techniques such as differential pulse voltammetry (DPV) [31], square wave voltammetry [32] and fast scan voltammetry [1] have been reported in the literature. UA and AA is co-present in biological fluids, it is important to develop a technique to selectively detect UA in the presence of AA conveniently in routine assay. However, the direct electro-oxidation of UA and AA at bare electrodes requires high overpotentials. The oxidation potentials of UA and AA are also too close therefore it is difficult to be separately determined by the use of bare electrodes. The ability to determine DA, AA and UA, which are present together in some biological tissues [33] selectivity in a mixture, is significant. At traditional solid electrodes, AA and UA are oxidized at potentials close to that of DA, resulting in an overlapping voltammetric response [34]. Several works in the literature like carbon ionic liquid electrode [35], orcet blue modified electrode [5] and ruthenium oxide modified electrode [36] reported for simultaneous determination of DA, AA and UA. But these methods have some disadvantage and drawbacks.

The surface modification of electrodes with metal nanoparticles has led to some latest developments of electrochemical sensors. Especially, platinum nanoparticles have evoked increasing interests in the design of sensors [37], and some reports have demonstrated that platinum nanoparticles can facilitate the electron transfer and increase the surface areas with enhanced mass transport characteristics [24]. Nanostructured platinum modified electrodes were prepared by electro deposition of platinum on nafion film coated glassy carbon (GC) electrode and electro catalytic oxidation of DA and serotonin done by GC/Nafion/nanoPt electrodes in the presence of interfering molecules such as AA and UA [38]. The determination of DA was done by using polymer matrix and gold nanoparticles [39]. Gold nanoparticles immobilized on amine-terminated self-assembled monolayers (SAM) on a polycrystalline Au electrode were successfully used for the selective determination of DA in the presence of ascorbate [40]. The poly(dimethylsiloxane) surface modification with gold nanoparticles used for the detection of DA and epinephrine [41]. Gold nanoparticles distributed poly(4-aminothiophenol) modified electrode [42] and 3-mercaptopropionic acid assembled on gold nanoparticle arrays were also reported [43]. L-Cysteine the additive plays an important role in self-assembled monolayers. Size and crystalline structure of gold nanoparticles was controlled by using L-Cysteine [44]. Ferrocene-Cysteine self-assembled supramolecular film modified electrode showed good catalytic activity for the oxidation of AA [45]. The bi-metallic hybrid film modified electrodes are important studies in the new era. Carbon-supported bi-metallic AuPt nanoparticles reported for electrocatalytic methanol oxidation [46], AuPt alloy nanoparticle catalysts in electrocatalytic reduction of oxygen was reported [47]. There were no reports in the bi-metallic hybrid film modified electrodes, to develop a sensor, which can determine DA, AA and UA simultaneously. In this article, for the first time, we are reporting PtAu hybrid film modified electrode with additive L-Cysteine for the simultaneous determination of DA, AA and UA. The electrochemical characterization of the PtAu hybrid film modified electrode was carried out using electrochemical quartz crystal microbalance (EQCM); the other analysis was carried out by using scanning electron microscopy (SEM), atomic force microscopy (AFM) and X-ray diffraction (XRD). The CV and DPV were used to study the electrocatalytic behavior and the simultaneous determination of ternary mixtures of DA, AA and UA.

2. Materials and methods

2.1. Instruments

Cyclic voltammetry (CV) and differential pulse voltammetry (DPV) were performed in an analytical system model CHI-410 and CHI-900 potentiostat, respectively. A BAS glassy carbon electrode (area = 0.07 cm^2) was used as the working electrode. A conventional three-electrode cell assembly consisting of an Ag/AgCl reference electrode and a platinum wire counter electrode was used for electrochemical measurements. The working electrode was either an unmodified glassy carbon electrode or a glassy carbon electrode modified with the PtAu hybrid films,

all the potentials were reported versus the Ag/AgCl reference electrode. The working electrode for EQCM measurements was an 8 MHz AT-cut quartz crystal coated with a gold electrode. The diameter of the quartz crystal was 13.7 mm; the gold electrode diameter was 5 mm. The morphological characterization of PtAu hybrid film was examined by means of SEM (Hitachi S-3000H), AFM (Being Nano-Instruments CSPM-4000) and XRD from Rigaku, Philips PW1729 Instrument.

2.2. Chemicals

K_2PtCl_6, $KAuCl_4{\cdot}3H_2O$, L-Cysteine, DA, AA and UA were of analytical grade and used without further purification. The solutions were prepared with double distilled water. DA, AA and UA solutions were prepared freshly and used. All the test solutions were deaerated by passing high purity nitrogen before the electrochemical experiment. The catalytic studies were carried out in potassium hydrogen phthalate (KHP) buffer of pH 4.0.

2.3. Preparation of PtAu hybrid film

Before modification, the glassy carbon electrode was polished using a BAS polishing kit with 0.05 μm alumina slurry, rinsed, ultrasonicated in double distilled deionized water. Hybrid film of PtAu were electro deposited onto the surface of glassy carbon electrode from 0.5 M H_2SO_4 solution containing K_2PtCl_6 (1×10^{-3} M), $KAuCl_4{\cdot}3H_2O$ (1×10^{-3} M) and 100 μM L-Cysteine in a potential range of 1.5 to −0.15 V, respectively. The number of cycles for all the experiments was 30. The concentration of L-Cysteine (100 μM) was exactly measured using micro-syringe.

3. Results and discussion

3.1. Electrochemical deposition of PtAu hybrid film

Hybrid films of PtAu were deposited onto the surface of a glassy carbon electrode from 0.5 M H_2SO_4 solution containing K_2PtCl_6 (1×10^{-3} M), $KAuCl_4{\cdot}3H_2O$ (1×10^{-3} M) and 100 μm L-Cysteine. Fig. 1A illustrates PtAu hybrid film formation from acidic medium on GC surface by CV. The forward scan was started at 1.5 V and scanned towards the negative direction up to −0.15 V. It exhibited four peaks corresponding to reduction of Au at 1.2 V, L-Cysteine (0.67 V), Pt (0.35 V) and for hydrogen adsorption at −0.1 V. On subsequent cycles, all the peaks were found growing. This result indicates that during the cycle, the deposition of platinum particle (Pt) and Au particles takes place on GC electrode. To confirm the hybrid nature of the film, separate Pt particle and Au particles deposition were performed. For Au particles deposition on GC electrode surface the potential range was between 1.1 and 0 V (Fig. 1B). It exhibited single peak corresponding to reduction of Au at 0.70 V. On subsequent cycles, the peak current increases and it is an indication of deposition of Au particles. For Pt particle deposition, the CV was performed between 1.1 and −0.2 V (Fig. 1C). The two peaks corresponding to reduction of Pt particle at 0.6 V, and hydrogen adsorption at −0.1 V were obtained [48]. On continuous cycle, all the peaks were found growing, which suggest that Pt particle deposition takes place on GC electrode surface. Comparing Fig. 1A–C, shows that the Pt particle and Au particles were present in the hybrid film. Here after the deposited Au particles will be called as nanoAu particles.

3.2. The electrochemical properties of PtAu hybrid film

Fig. 1D shows the CV of PtAu hybrid film modified electrodes in deaerated KHP (potassium hydrogen phthalate, pH 4.0) buffer at different scan rates. It shows that the film on a GC electrode has two cathodic peaks at 0 and 0.6 V. The peak currents of these peaks increase linearly with scan rates upto 500 mV s^{-1}. The results showed that the PtAu hybrid film was stable and electrochemically active in KHP solution. Further the reduction peaks of Pt particle and nanoAu shifts to more negative side at higher scan rates. The inset of Fig. 1D shows a plot of the cathodic peak current versus scan rate that showed a close linear dependence with the scan rate. The linear line indicates the reversible, diffusionless electron transfer process of Pt particle (A) and nanoAu (B) with a proton exchange, respectively. Additionally, the voltammetric data were subjected to analysis by plotting $\log(i_p)$ versus $\log(v)$ the scan rate (data not shown) and the expected the slope value obtained was near to one. From these result, it shows that the PtAu hybrid film was a monolayer film. Furthermore, Fig. 2 shows the cyclic voltammetric response of PtAu hybrid film formation in presence of L-Cysteine (Fig. 2b and c) at 100 and 500 mV s^{-1}. Fig. 2a shows the cyclic voltammetric response of PtAu hybrid film in absence of L-Cysteine. Here, comparing these results, shows that the additive L-Cysteine plays an important role for such kind of film formation. Without L-Cysteine, the adherence of the Pt and nanoAu particles were not stable (Fig. 2a). So the presence of L-Cysteine helps to bound the Pt and nanoAu particles onto the electrode surface.

3.3. EQCM measurements of PtAu hybrid film, platinum and nanoAu particles

EQCM is a powerful technique capable of detecting very small mass changes at the electrode surface that accompanies any electrochemical process. The EQCM and CV were used to study the in situ growth of the PtAu hybrid film. Fig. 3A shows the consecutive CV of a PtAu hybrid film on a gold electrode. The CV of the PtAu hybrid film was obtained from 0.5 M H_2SO_4 solution containing K_2PtCl_6 (1×10^{-3} M), $KAuCl_4{\cdot}3H_2O$ (1×10^{-3} M) and 100 μm L-Cysteine. Fig. 3B shows the change in the EQCM frequency recorded during the first seven cycles of consecutive CVs. The increase in the voltammetric peak current in Fig. 3A and the decrease in frequency (or increase in mass) in Fig. 3B were found consistent with the growth of a PtAu hybrid film on the gold electrode. These results showed that the deposition potential was obviously between 1.5 and −0.15 V (versus Ag|AgCl). In the EQCM experiment, the mass change at the gold electrode from the frequency change (assuming the film to be a rigid resonator) was derived from the

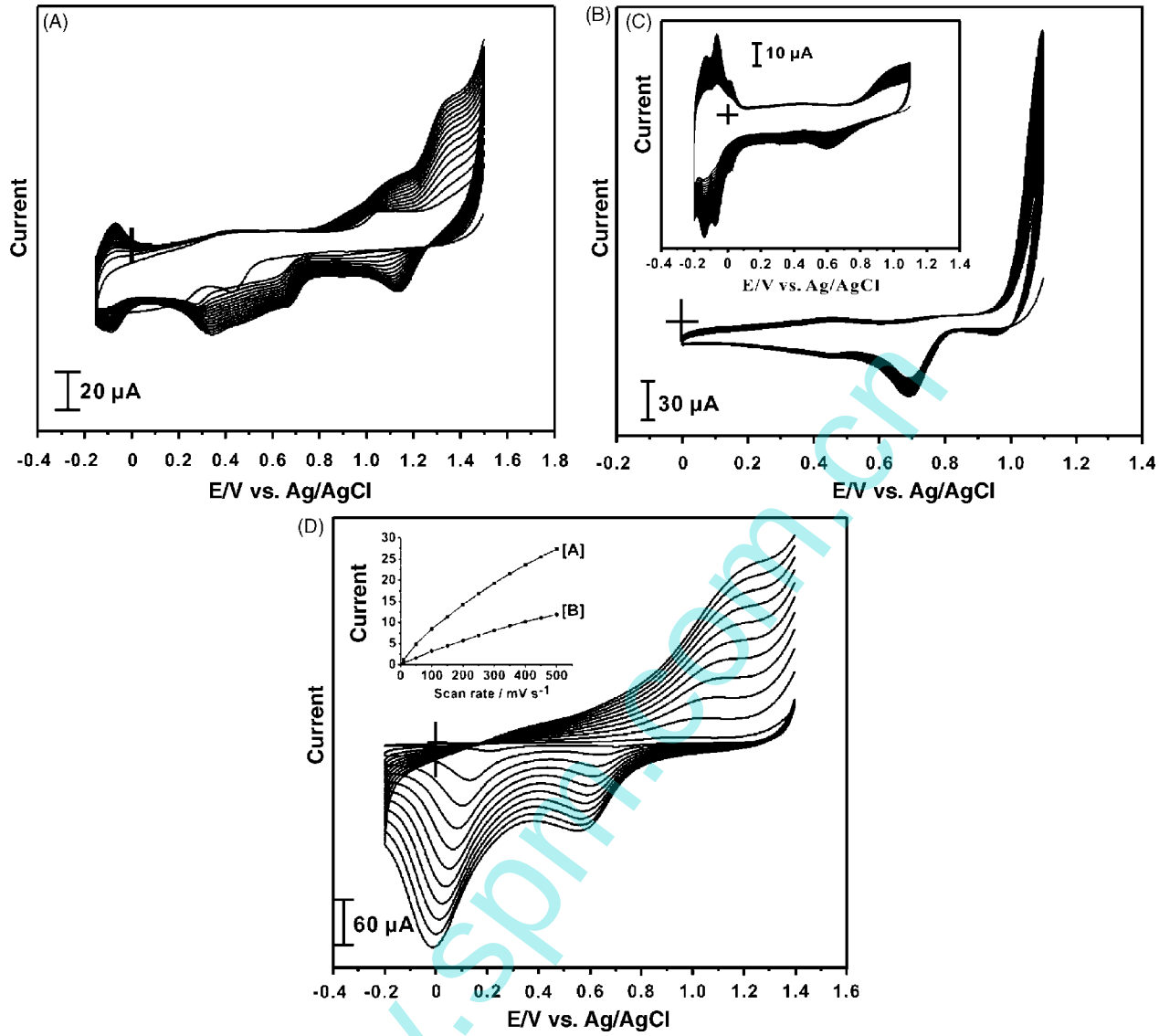

Fig. 1. Repeated cyclic voltammograms for the deposition of (A) PtAu hybrid film from 0.5 M H_2SO_4 containing 1×10^{-3} M $KAuCl_4 \cdot 3H_2O$ and 1×10^{-3} M K_2PtCl_6 with 100 μM L-Cysteine, (B) Au particles from in 0.5 M H_2SO_4 containing 1×10^{-3} M $KAuCl_4 \cdot 3H_2O$, (C) Pt particles from 1×10^{-3} M K_2PtCl_6 in 0.5 M H_2SO_4. Scan rate = 0.1 V/s. (D) Cyclic voltammetric response of PtAu hybrid film modified electrode in 0.1 M KHP buffer (pH 4.0) at different scan rates: (a) 10, (b) 50, (c) 100, (d) 150, (e) 200, (f) 250, (g) 300, (h) 350, (i) 400, (j) 450 and (k) 500 mV s^{-1}. Inset shows the plot of cathodic peak current of platinum (A) and gold (B) vs. scan rate.

Sauerbrey equation [49,50].

$$\text{mass change}\,(\Delta m) = -\frac{1}{2}(f_0^{-2})(\Delta f)A(k\rho)^{1/2},$$

where Δf is the observed frequency change, A the area of the gold disk coated onto the quartz crystal, ρ the density of the crystal, k the shear modulus of the crystal and f_0 is the oscillation frequency of the crystal. Here, 1 Hz frequency change is equivalent to 1.4 ng mass change. During the first CV scan, about 719.78 ng/cm^2 of PtAu hybrid film was deposited on the gold electrode and a total of about 5038.47 ng/cm^2 of PtAu hybrid film was deposited after the seventh scan cycle. The inset shows the plot of frequency change versus the scan cycle (no. of cycles during the film formation) and this curve was linear as expected. Similar experiments carried out for individual deposition of Pt and Au particles. In the case of Pt, first scan, about 392.37 ng/cm^2 of Pt particle was deposited on the gold electrode and a total of about 9024.69 ng/cm^2 of Pt particle was deposited after 23 scan cycles (figures not shown). For nanoAu, about 635.78 ng/cm^2 of nanoAu film was deposited in the first scan and a total of about 6357.82 ng/cm^2 of nanoAu was deposited at the end of 10 scan cycles (figures not shown). As expected, the Sauerbrey relation, the plot of frequency change versus the number of scan (figures not shown) was linear.

3.4. SEM characterization of Pt particle, nanoAu and PtAu hybrid film

The surface morphologies of Pt, nanoAu and PtAu hybrid film modified electrode were studied by SEM and the results are shown in (Fig. 4A–F). From the SEM images, it shows that the Pt

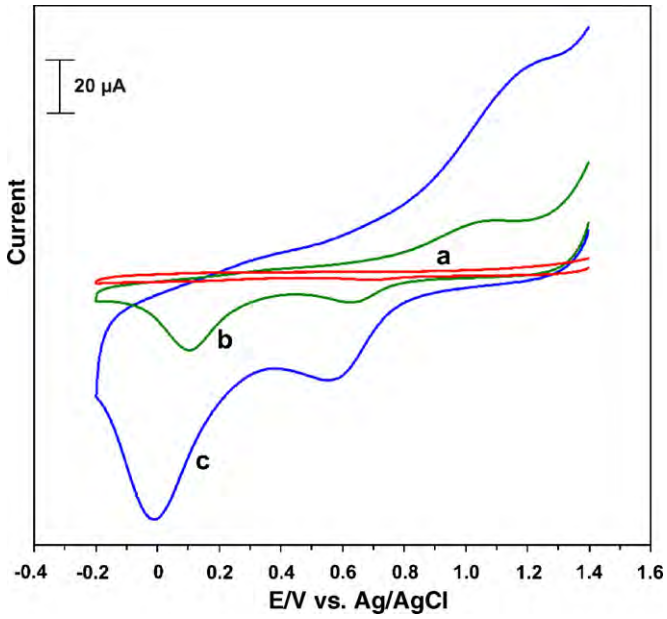

Fig. 2. Cyclic voltammetric response of PtAu hybrid film modified electrode in 0.1 M KHP buffer (pH 4.0) in (a) absence of L-Cysteine (100 mV s^{-1}), (b) presence of L-Cysteine (100 mV s^{-1}) and (c) presence of L-Cysteine (500 mV s^{-1}).

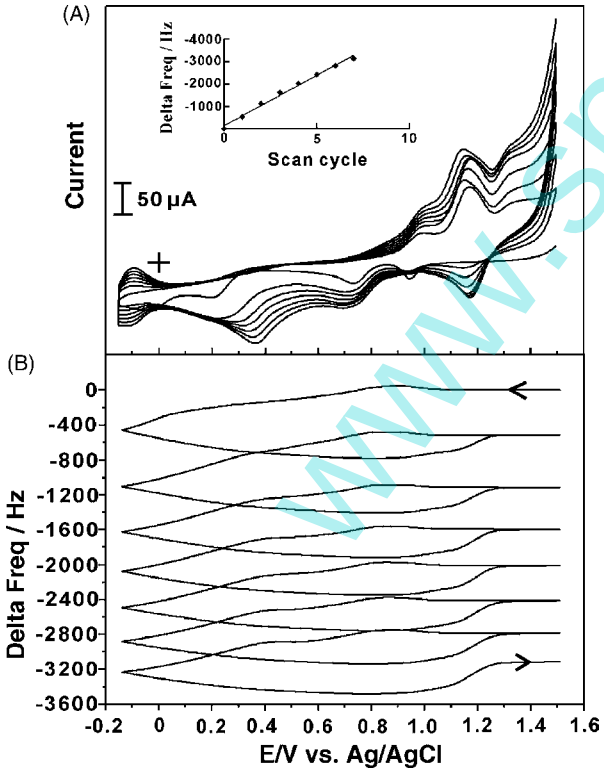

Fig. 3. (A) Repeated cyclic voltammograms of gold electrode modified with PtAu hybrid film from 0.5 M H_2SO_4 containing 1×10^{-3} M $KAuCl_4 \cdot 3H_2O$ and 1×10^{-3} M K_2PtCl_6 with 100 μM L-Cysteine. (B) The change in EQCM frequency was recorded concurrently with the first seven consecutive cyclic voltammograms between −0.15 and 1.5 V. The inset shows total frequency change ΔF vs. scan cycle.

particles dispersed homogeneously and appear as bright, round shaped particles adhering to the electrode surface (Fig. 4A). The SEM image indicates the size distribution of Pt particles varies from 200 to 300 nm (SEM view angle 60°). The Pt particle size was bigger and visually distinguishable. Here, the Pt particle size falls in slight higher dimension (200–300 nm), so it was represented as Pt particle. Even though it falls in higher dimension, it exhibits the nanoproperties along with the nanoAu particles. In addition, Fig. 4B shows that the nanoAu particles were finely adhered on the electrode and the nanoAu particles appear as homogeneous dispersion and the size were smaller than the Pt particles (50–80 nm) (SEM view angle 60°). In the PtAu hybrid film (Fig. 4C–F), we can easily distinguish both the Pt particles and nanoAu particles by its size and shape variation. It was confirmed that the bi-metallic Pt and nanoAu particles deposited as a monolayer film. Here, the simultaneous deposition of Pt particles and nanoAu is the important one. The L-Cysteine, the additive plays an important role here for the simultaneous deposition of Pt particles and nanoAu Particles.

As shown in Fig. 4C–F, the spherical shaped Pt particles were randomly deposited with nanoAu nanoparticles. Fig. 4C and D show the SEM image of a PtAu hybrid film. Comparison of Fig. 4C and D, which were corresponding to PtAu hybrid film deposited on indium tin oxide (ITO) for 30 and 60 cycles, respectively, shows that the increasing cycle does not change the particle size and structure, but the increasing cycles will result in the more deposition of particles onto the ITO surface. In PtAu hybrid film the morphology is similar to that of Pt particle, nanoAu obtained separately (Fig. 4A and B). Fig. 4E shows the PtAu hybrid film obtained from 30 cycles (view angle 60°) and Fig. 4F shows the PtAu hybrid film from 60 cycles (view angle 60°). From these images, it revealed that robust and uniform structure and from the different view angle we can see very clear images of the PtAu hybrid film. The results were similar when repeating the electrodeposition process under the same conditions, indicating that the PtAu hybrid film deposited on the ITO surface have a good reproducibility. From these result and comparison with Pt, nanoAu particle, the PtAu hybrid film was confirmed.

3.5. AFM characterization of PtAu hybrid film

The PtAu hybrid film was characterized by using atomic force microscopy in tapping mode. The scanning area of the film was 7 μM × 7 μM. The AFM images of ITO electrode surface formed under the electrodeposition of PtAu hybrid film for 30 potential cycles (Fig. 5). Fig. 5A depicts the topographic image of the PtAu hybrid film (30 potential cycles). For 30 potential cycles more isolated and clear topographic image was obtained. From the topographic image, we can easily distinguish the Pt and nanoAu particles. Here, the spherical shaped and big size particles were Pt and the small size particles were nanoAu, respectively. However, for 60 potential cycles the density of the Pt and nanoAu particles were increased (figure not shown), but the together coagulations does not take place. Here, the particle growth spread over the electrode surface. From the topographic and three-dimensional image, it reveals that

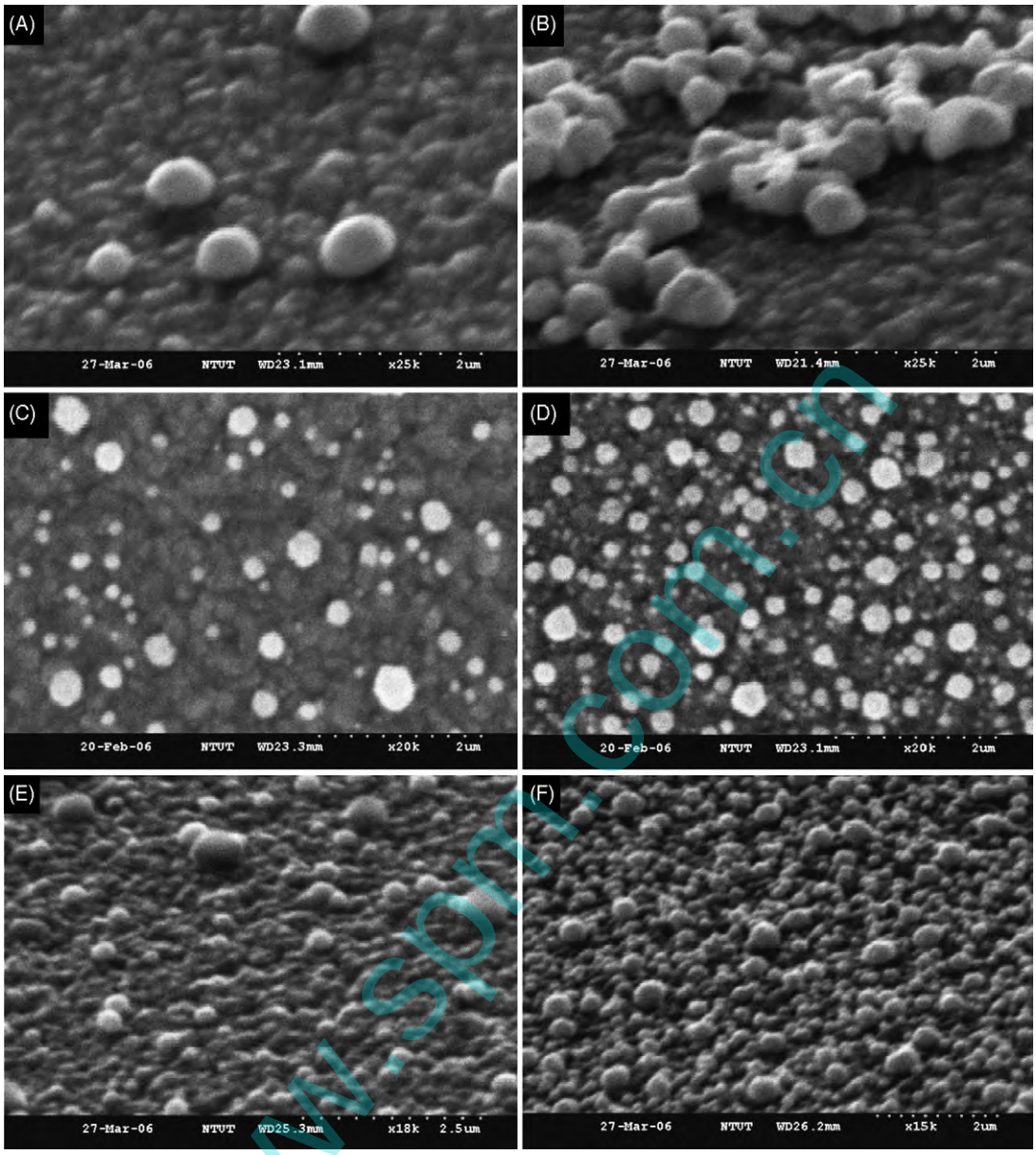

Fig. 4. (A) SEM images of the Pt particles deposited on ITO from 0.5 M H_2SO_4 containing 1×10^{-3} M K_2PtCl_6 (magnification 25 K, view angle 60°). (B) NanoAu particles deposited on ITO from 0.5 M H_2SO_4 containing 1×10^{-3} M $KAuCl_4 \cdot 3H_2O$ (magnification 25K, view angle 60°). (C) PtAu hybrid film deposited on ITO from 0.5 M H_2SO_4 containing 1×10^{-3} M $KAuCl_4 \cdot 3H_2O$ and 1×10^{-3} M K_2PtCl_6 (100 μM L-Cysteine, magnification 20K, 30 cycles). (D) PtAu hybrid film (magnification 20K, 60 cycles). (E) PtAu hybrid film (magnification 20K, 30 cycles, 60°). (F) PtAu hybrid film (magnification 20K, 60 cycles and 60°).

the uniformed spherical shape structures of Pt, nanoAu structure were confirmed [51,52]. The three-dimensional view of the same film (Fig. 5B) and cross-sectional profile analysis (graph) illustrates that the minimum and maximum spherical sizes of the Pt and nanoAu particle were in the range of 200–300 and 50–80 nm, respectively. The morphological characteristics of Pt, nanoAu particles observed from the AFM images were consistent with their SEM images, clearly showing a monolayer film consist of both Pt, nanoAu particles in different size range. According to these results, it can be concluded that the monolayer film consists of both Pt and nano size Au particles. From Fig. 5, it confirms the size variation and the differentiation of the particles on the electrode surface and the Pt, nanoAu particles were more nearly uniform size, the density of the Pt particles was highest than the nanoAu particle.

3.6. XRD studies

The XRD analysis was used to characterize the crystal structure of the resulting platinum and gold nano particles and further demonstrated the nanostructures. The PtAu hybrid film was obtained by cycling the ITO surface between the potential range of 1.5 and −0.15 V in a solution containing 1×10^{-3} M $KAuCl_4 \cdot 3H_2O$ and 1×10^{-3} M K_2PtCl_6 in 0.5 M H_2SO_4 (100 μM L-Cysteine) for 30 cycles. As shown in Fig. 6, XRD peak appeared at 2θ of 39.7°, 46°, 62.5°, 78.8°, which can be assigned to the diffraction (1 1 1), (2 0 0), (2 2 0), (3 1 1)

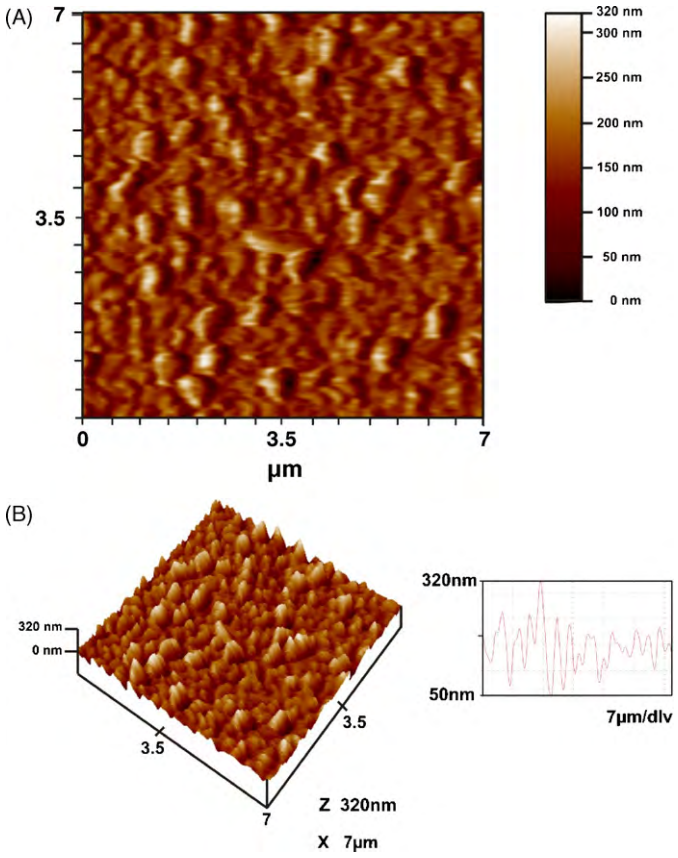

Fig. 5. (A) Topographic view of PtAu hybrid film deposited on ITO from 0.5 M H_2SO_4 containing 1×10^{-3} M $KAuCl_4 \cdot 3H_2O$ and 1×10^{-3} M K_2PtCl_6 (100 μM L-Cysteine, 30 cycles). (B) Three-dimensional view and cross-sectional graph of the above film.

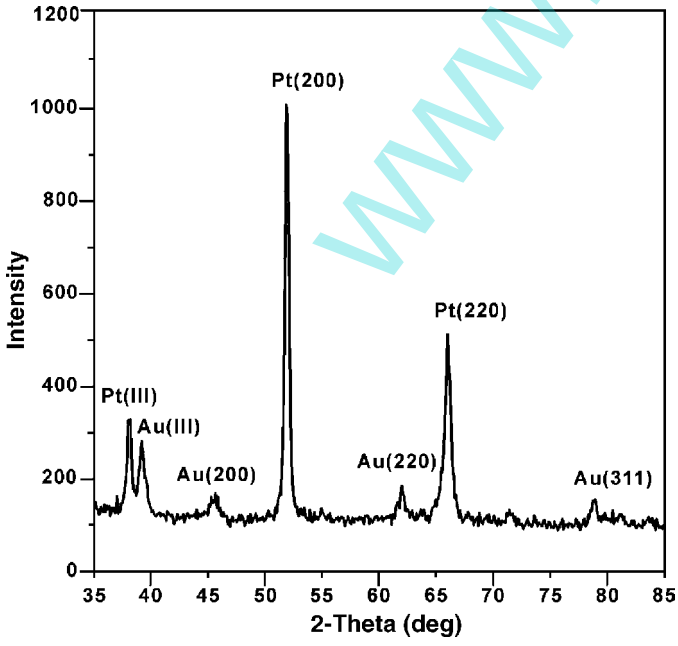

Fig. 6. XRD spectra of the PtAu hybrid film on ITO.

Table 1
Comparison table for the electro catalytic activity for AA, DA and UA individually in CV on PtAu hybrid film modified GC, bare GC in 0.1 M KHP buffer (pH 4.0) aqueous solution

Analyte	Type of electrode	E_{pa} (V)	I_{pa} (μA)
AA oxidation	Bare electrode	0.62	11.07
	PtAu hybrid film modified electrode	0.19	21.66
DA oxidation	Bare electrode	0.53	4.62
	PtAu hybrid film modified electrode	0.35	9.58
UA oxidation	Bare electrode	0.54	7.13
	PtAu hybrid film modified electrode	0.52	10.85

AA concentration = 7.044×10^{-4} M; DA concentration = 3.12×10^{-4} M; UA concentration = 9.992×10^{-4} M.

structure of the face-centered cubic (fcc) nano metal gold structures, respectively [53,54]. For Pt particle, it clearly shows the three main characteristic peaks of the face-centered cubic (fcc) crystalline Pt and has major peaks at (1 1 1) at 38°, (2 0 0) at 53°, (2 2 0) at 66° indicating the successful reduction of metal salt to Pt particles [55,56]. The XRD results reveal that nanoAu particle were in the range 50–80 nm and platinum particle in the range of 200–300 nm, respectively. The particle size value calculated from XRD using Scherrer formula [57] is in good agreement with the size value obtained from SEM and AFM observation.

3.7. Individual catalytic oxidation of AA, DA and UA

The electro catalytic oxidation of DA, AA and UA on the GC electrode was investigated by CV. Table 1 shows the individual catalytic oxidation potential and current of AA, DA and UA, respectively. Here, the DA oxidation, at bare electrode takes place at 0.53 V, but for PtAu hybrid film modified electrode the potential shift to 0.35 V with much enhanced anodic peak current from 11.07 to 21.66 μA. On the other hand, for AA oxidation the potential shifts to the less potential (0.19 V) comparing with bare electrode 0.62 V. In the case of UA, the oxidation takes place at 0.54 V at bare electrode and for PtAu hybrid film it occurred at 0.52 V. The potential shift and current increase shows the good catalytic activity of PtAu hybrid film modified electrode on the individual electro catalytic oxidation of AA, DA and UA.

3.8. Simultaneous catalytic oxidation of AA, DA and UA

The main aim of the present investigation is to determine the AA, DA and UA simultaneously. The simultaneous determination of DA, AA and UA mixture (Fig. 7A), at the bare electrode fails to separate the three peaks, shows a broad peak at 0.6 V. But at film modified electrode, three clear and well separated peaks at 0.25 V for AA, 0.37 for DA and 0.54 V for UA were observed. The mechanism behind the oxidation of AA, DA and UA at a wide potential separation in the modified electrodes may be due to the multivalent nature of the electrode. Oxidation currents are increased linearly on increasing the concentration of AA, DA and UA. The linear range of the concentration for the determination of AA, DA and UA using CV were 0.069–1.384, 0.022–0.44 and 0.062–2.499 mM, respectively. The AA and UA

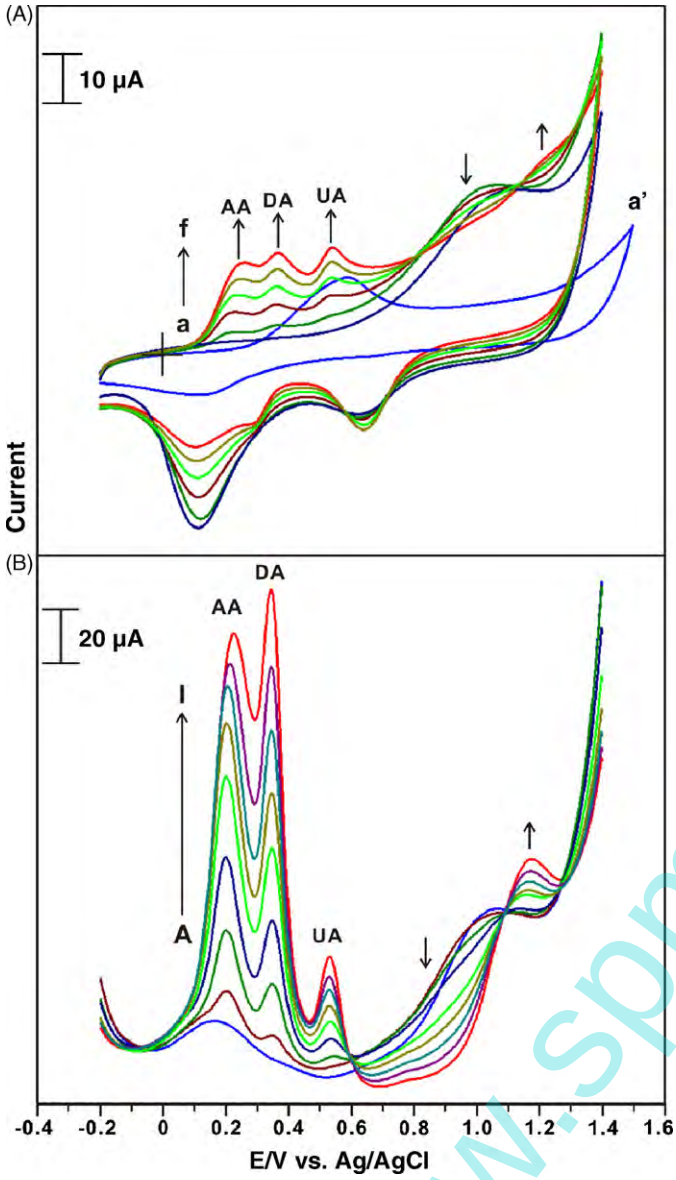

Fig. 7. (A) Cyclic voltammograms of the PtAu hybrid film modified electrode in 0.1 M KHP buffer (pH 4.0) containing individual concentrations of AA, DA and UA mixture. [AA]: 0.0, 0.069, 0.346, 0.692, 1.038 and 1.384 mM. [DA]: 0.0, 0.022, 0.110, 0.220, 0.330 and 0.440 mM; [UA]: 0.0, 0.062, 0.312, 1.249, 1.874 and 2.499 mM. (a′) bare GC [AA, DA, UA]: 1.384, 0.44 and 2.499 mM. (B) Differential pulse voltammograms of AA, DA and UA mixture at PtAu hybrid film at GC in 0.1 M KHP (pH 4.0) aqueous solution containing individual concentration of AA (from A to I): 0.0, 0.103, 0.206, 0.413, 0.619, 0.826, 1.03, 1.23, 1.44 and 1.65 mM; [DA] (from A to I): 0.0, 0.024, 0.048, 0.096, 0.144, 0.192, 0.240, 0.280, 0.336 and 0.384 mM; [UA] (from A to I): 0.0, 0.021, 0.042, 0.084, 0.126, 0.168, 0.210, 0.252, 0.294 and 0.336 mM.

which are in the mM level in biological fluids interfere the determination. By using PtAu hybrid film modified electrode we can see well separated peaks for AA, DA and UA in milli molar level concentration. From the results, it is clear that the PtAu hybrid film modified electrode shows very obvious anodic peak currents for AA, DA and UA separately. Scheme 1 could explain the electron mediating properties of PtAu hybrid film towards the oxidation of DA, AA and UA. Here, the nanoAu exhibited one additional oxidation peak at potential about +1.2 V. On addition of AA, DA, UA or mixture, the oxidation peak current of Au was increased. Here, the oxidation of DA, AA, UA, or mixture mediated by oxidized form of Au present in the solution. So this phenomenon attributed to the mediated oxidation reaction of oxidation state of Au towards DA, AA, UA or mixture.

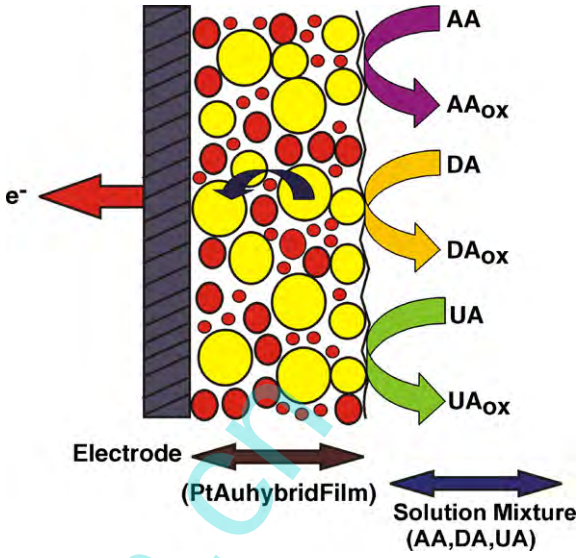

Scheme 1. Schematic representation of the simultaneous electro catalytic oxidation of DA, AA and UA by PtAu hybrid film modified electrode.

3.9. DPV studies

For simultaneous determination of DA, AA and UA, DPV was carried out in the potential range of −0.2 to 1.4 V (pH 4.0) (Fig. 7B). The DPV results shows that the simultaneous determination of DA, AA and UA with well separated three anodic peaks corresponding to their oxidation could be possible at PtAu hybrid film modified electrode. The presence of PtAu hybrid film on the GC electrode resolved the mixed voltammetric responses into three well-defined voltammetric peaks at potentials 0.2, 0.35 and 0.54 V, corresponding to the oxidation of DA, AA and UA, respectively. Peak separations of 0.15 and 0.19 V between DA and AA and DA and UA, respectively, allow us to detect DA, AA and UA simultaneously by using DPV. Similar results were obtained at gold nanoparticles modified electrode [42]. Here, the separation between the three peak potentials is sufficient enough for the determination of the three species of AA, DA and UA. In addition, a substantial increase in peak currents was also observed due to the reversibility of the electron transfer process. The linear range of the concentration for the determination of AA, DA and UA using DPV were 0.103–1.65, 0.024–0.384 and 0.021–0.336 mM, respectively. The slopes of the linear calibration curves between the peak current and the concentration were estimated to be 0.0083, 0.05 and 0.0152 μA μM^{-1} for AA, DA and UA, respectively. The correlation coefficient of AA, DA and UA were found 0.9906, 0.9983 and 0.9875. The relative standard deviation (% R.S.D., $n = 10$) for AA (1.65 mM), DA (0.384 mM) and UA (0.336 mM) using DPV were 1.363%, 1.207% and 1.88%, respectively. In DPV, we also get two peaks additionally at 1.1 and 1.2 V indicates the platinum oxide and

gold oxide, respectively. The platinum oxide peak decreases and the oxidation peak of nanoAu increasing because the nanoAu exhibited one additional oxidation peak at potential about 1.2 V. This is due to the mediated oxidation reaction of oxidation state of Au towards AA, DA and UA mixture.

Fig. 8A exhibits the DPV that were obtained for the different concentrations of DA and UA (a–e) in the presence of 1.033 mM concentration of AA. The slopes of the linear calibration curves between the peak current and the concentration were estimated to be 0.0499, 0.0156 $\mu A\ \mu M^{-1}$ for DA and UA, and the correlation coefficient is 0.9959, 0.9856, respectively. Here, the AA peak decreases due to the increasing concentration of the DA and UA. This is due to increasing concentration of DA and UA in presence of higher concentration of AA, will increase the anodic peak currents of the DA and UA with decreasing peak current of the AA. Fig. 8B shows the DPV that were obtained from the different concentration of the AA and UA in presence of very low concentration (0.024 mM) of DA. The peak current increases with the increasing concentration of the AA and UA mixture. Here, the concentration of AA and UA varies from 0.309 to 1.126 mM, 0.0749–0.276 mM, respectively. From these results, it can be concluded that for very low concentration detection of DA and UA in high concentration of AA is possible. The slopes of the linear calibration curves between the peak current and the concentration were estimated to be 0.0079, 0.0625 $\mu A\ \mu M^{-1}$ for AA and DA, respectively. The correlation coefficient of AA and DA were found 0.9280, 0.9986, respectively. On the other hand, Fig. 8C depicts the DPV voltammograms of different concentration of AA and DA in presence of 4.8 mM of UA. Here, the concentration of DA ranges from 0.168 to 0.240 mM and UA concentration varies from 0.723 to 1.03 mM. The slopes of the linear calibration curves between the peak current and the concentration were estimated to be 0.0499, 0.0156 $\mu A\ \mu M^{-1}$ for DA, UA and the correlation coefficient were found 0.9959, 0.9856, respectively. It is interesting to note that the sensitivities of the modified electrode toward AA and DA are approximately same in the higher concentration of UA which indicates the facts that the oxidation processes of DA, AA and UA at PtAu hybrid film modified electrode surface were independent and therefore simultaneous or independent measurement of the three analyte were possible without any interference and it is suitable to detect the samples with less or equal concentration. From the CV and DPV, it can be concluded that the PtAu hybrid film is good for the wide range of the concentration variation. These detection limits are low enough for the application of analysis in PtAu hybrid film modified glassy carbon electrode for the simultaneous determination of AA, DA and UA. Table 2 illustrates the comparison of response characteristics of the proposed modified electrode with other modified electrodes reported in the literature for simultaneous determination of DA, AA and UA.

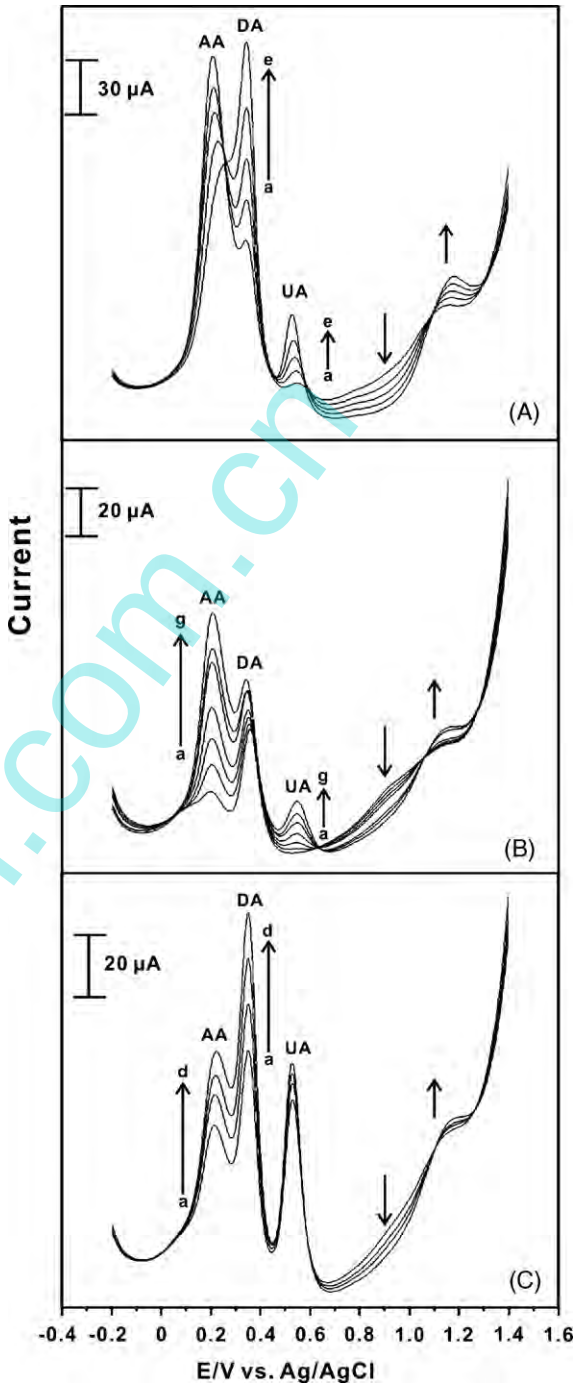

Fig. 8. Differential pulse voltammograms of (A) DA and UA in the presence of 1.033 mM AA in 0.1 M KHP (pH 4.0). DA and UA concentrations (from a to e); [DA] 0.121, 0.169, 0.218, 0.266 and 0.315 mM, [UA] 0.124, 0.174, 0.224, 0.274, 0.324 and 0.399 mM. (B) AA and UA in the presence of 0.24 mM DA in 0.1 M KHP (pH 4.0). AA and UA concentrations (from a to g) [AA]: 0.309, 0.413, 0.516, 0.619, 0.723, 0.923 and 1.126 mM: [UA] 0.0749, 0.099, 0.124, 0.149, 0.174, 0.224 and 0.276 mM. (C) DA and AA in the presence of 4.8 mM UA in 0.1 M KHP (pH 4.0). DA and UA concentrations from (a to d) [DA]: 0.168, 0.192, 0.216 and 0.240 mM; [AA] 0.723, 0.826, 0.929 and 1.03 mM.

3.10. Real sample analysis

The possibility of using PtAu hybrid film modified electrode for the determination of DA, AA and UA in practical samples such as DA injection solution, vitamin C tablets and human urine samples were tested. Here, the DPV technique was used in the experiments. The real sample analysis data for dopamine injection solution (DOPAMIN, 40 mg/ml), vitamin C tablets and human urine samples results were listed in Tables 3–5. From these results, it shows that the PtAu hybrid film modified elec-

Table 2
Comparison table for the different modified electrodes

Ref.	Linear range			Sensitivity ($\mu A\ \mu M^{-1}$)			$E_{p,a}$ (V)		
	AA	DA	UA	AA	DA	UA	AA	DA	UA
[42]	25 μM	25 μM	25 μM	–	–	–	0.01	0.21	0.47
[58]	150–1000 μM	20–200 μM	10–130 μM	0.016	0.228	0.091	0.18	0.32	0.50
[59]	0.075–0.187 mM	0.075–0.18 mM	0.75–0.18 mM	0.028	0.146	0.08	0.17	0.34	0.48
This work	0.103–0.165 mM	0.024–0.384 mM	0.02–0.336 mM	0.008	0.05	0.015	0.20	0.35	0.54

Table 3
Determination of DA in dopamine hydrochloride injection

Dopamine			
S.no.	Added (10^{-5} M)	Found (10^{-5} M)	Recovery (%)
1	1.16	1.20	103.0
2	2.32	2.45	105.0
3	3.48	3.30	94.8
4	4.64	4.50	96.9
5	5.80	5.75	99.0

Table 4
Determination of vitamin C

Vitamin C			
S.no.	Added (10^{-4} M)	Found (10^{-4} M)	Recovery (%)
1	4.14	3.90	94.20
2	5.52	5.54	100.36
3	6.90	7.13	103.33
4	8.28	8.27	99.98
5	9.66	9.65	100.57

Table 5
Human urine sample analysis

Human urine sample			
S.no.	Added (10^{-4} M)	Found (10^{-4} M)	Recovery (%)
1	1.24	1.18	95.16
2	2.48	2.40	96.77
3	3.72	3.80	102.0
4	4.96	4.98	100.40
5	6.20	6.0	96.70

trode shows good catalytic activity for real sample analysis and the obtained recoveries were satisfactory.

4. Conclusions

In this present work, we have constructed PtAu hybrid film electrode by using potassium hexachloroplatinate, potassium tetrachloroaurate and L-Cysteine by electro deposition method. The characterization of PtAu hybrid film has been highlighted by analytical methods like EQCM, SEM, AFM, XRD and electrochemical methods. The particle size of Pt and nanoAu were in the range of 200–300, 50–80 nm. Excellent linear correlation between AA, DA and UA oxidation current response were found up to the concentration of 1.65, 0.384 and 4.8 mM, respectively. PtAu hybrid film modified electrode showed efficient electro catalytic functions towards the simultaneous oxidation of DA, AA and UA. The anodic peak current increased remarkably for the injection of mixture of DA, AA and UA solution at PtAu hybrid film modified electrode. Large peak separations between AA, DA and UA allow the detection and determination of AA, DA and UA simultaneously at PtAu hybrid film by using CV or DPV. In DPV determination, the lower limit of detection of AA, DA and UA was estimated to be in the order of 0.103, 0.024 and 0.021 mM respectively. The % R.S.D. ($n = 10$) for AA (1.65 mM), DA (0.384 mM) and UA (0.336 mM) using DPV were 1.363%, 1.207% and 1.88%, respectively. The modified electrode not only improved the electrochemical catalytic oxidation of DA, AA and UA, but also resolved the overlapping anodic DA, AA and UA peaks into three well-defined peaks. No interference was observed between AA, DA and UA. So the PtAu hybrid film modified electrode is found to be effective for the construction of sensitive and stable biosensor for simultaneous determination of AA, DA and UA. Typical applications of PtAu hybrid film modified electrode towards estimating AA, DA and UA in real samples have been attempted. For the future prospective of this investigation is to be reducing the size of the platinum particle and increasing the sensitivity towards the neurotransmitters.

Acknowledgments

This work was supported by grants from National Science Council (NSC) and the Ministry of Education of the Taiwan (ROC).

References

[1] B.J. Venton, R.M. Wightman, Anal. Chem. 75 (2003) 414A–421A.
[2] K.-H. Xue, F.-F. Tao, S.-Y. Yin, W. Shen, W. Xu, Chem. Phys. Lett. 391 (2004) 243–247.
[3] L.R. Junior, J.C.B. Fernandes, G.O. Neto, J. Electroanal. Chem. 481 (2000) 34–41.
[4] R.P.H. Nikolajsen, A.M. Hansen, Anal. Chim. Acta 449 (2001) 1–15.
[5] H.R. Zare, N. Rajabzadeh, N. Nasirizadeh, M.M. Ardakani, J. Electroanal. Chem. 589 (2006) 60–69.
[6] G.-P. Jin, X.-Q. Lin, J.-M. Gong, J. Electroanal. Chem. 562 (2004) 135–144.
[7] M. Ferreira, L.R. Dinelli, K. Wohnrath, A.A. Batista, O.N. Oliveira Jr., Thin Solid Films 446 (2004) 301–306.
[8] K. Hayashi, Y. Iwasaki, R. Kurita, K. Sunagawa, O. Niwa, Electrochem. Commun. 5 (2003) 1037–1042.
[9] R. Kataky, E. Morgan, Biosens. Bioelectron. 18 (2003) 1407–1417.
[10] R.D. Shankaran, N. Uehara, T. Kato, Anal. Chim. Acta 478 (2003) 321–327.

[11] M.D. Pilar, T. Sotomayor, A.A. Tanaka, L.T. Kubota, Anal. Chim. Acta 455 (2002) 215–223.
[12] L. Mao, K. Yamamoto, Anal. Chim. Acta 415 (2000) 143–150.
[13] F. Lisdat, U. Wollenberger, A. Makower, H. Hçrtnagl, D. Pfeiffer, F.W. Scheller, Biosens. Bioelectron. 12 (1997) 1199–1211.
[14] M.A. Dayton, A.G. Ewing, R.M. Wightman, J. Electroanal. Chem. 146 (1983) 189–200.
[15] S. Hrapovic, Y.L. Liu, K.B. Male, J.H.T. Luong, Anal. Chem. 76 (2004) 1083–1088.
[16] B. Nalini, S.S. Narayanan, Anal. Chim. Acta 405 (2000) 93–97.
[17] S.S.L. Castro, V.R. Balbo, P.J.S. Barbeira, N.R. Stradiotto, Talanta 55 (2001) 249–254.
[18] I.G. Casello, M.R. Guascito, Electroanalysis 9 (1997) 1381–1386.
[19] A.M. Yu, H.-L. Zhang, H.-Y. Chen, Electroanalysis 9 (1997) 788–790.
[20] P.R. Roy, T. Okajima, T. Ohsaka, Bioelectrochemistry 59 (2003) 11–19.
[21] Z. Gao, K.S. Siow, A. Ng, Y. Zhang, Anal. Chim. Acta 343 (1997) 49–57.
[22] L. Zhang, X. Lin, Analyst 126 (2001) 367–370.
[23] R.N. Goyal, N.K. Singhal, Bioelectrochem. Bioener. 44 (1998) 201–208.
[24] Y. Kariyana, S. Yamauchi, T. Yukiashi, H. Ushioda, Anal. Lett. 20 (1987) 1791–1801.
[25] F. Mizutani, Y. Sato, Y. Hirata, S. Iijima, Anal. Chim. Acta 441 (2001) 175–181.
[26] D. Martinoz-Perez, M.L. Ferrer, C.R. Mateo, Anal. Biochem. 322 (2003) 238–242.
[27] Y. Chen, T.C. Tan, Talanta 42 (1995) 1181–1188.
[28] J. Wang, P. Tuzhi, T. Golden, Anal. Chim. Acta 194 (1987) 129–138.
[29] R.D. Shankaran, K. Iimura, T. Kato, Sens. Actuat. B 94 (2003) 73–80.
[30] M. Kooshki, E. Shams, Anal. Chim. Acta 587 (1) (2007) 110–115.
[31] H.S. Wang, T.H. Li, W.L. Jia, H.Y. Xu, Biosens. Bioelectron. 22 (2006) 582–588.
[32] C.R. Raj, K. Tokuda, T. Ohsaka, Bioelectrochemistry 53 (2001) 183–191.
[33] Y. Zhang, G. Jin, Y. Wang, Z. Yang, Sensors 3 (2003) 443–450.
[34] A. Salimi, H. Mam-Khezri, R. Hallaj, Talanta 70 (2006) 823–832.
[35] A. Safavi, N. Maleki, O. Moradlou, F. Tajabadi, Anal. Biochem. 359 (2006) 224–229.
[36] P. Shakkthivel, S.-M. Chen, Biosens. Bioelectron. 22 (2006) 1680–1687.
[37] J.-B. Raoof, R. Ojani, S.R. Nadimi, Electrochim. Acta 50 (2005) 4694–4698.
[38] T. Selvaraju, R. Ramaraj, J. Electroanal. Chem. 585 (2005) 290–300.
[39] S. Senthil Kumar, J. Mathiyarasu, K.L.N. Phani, J. Electroanal. Chem. 578 (2005) 95–103.
[40] C. Retna Raj, T. Okajima, T. Ohsaka, J. Electroanal. Chem. 543 (2003) 127–133.
[41] A.-J. Wang, J.-J. Xu, Q. Zhang, H.-Y. Chen, Talanta 69 (2006) 210–215.
[42] A.I. Gopalan, K.-P. Lee, K.M. Manesh, P. Santhosh, J.H. Kim, J.S. Kang, Talanta 71 (4) (2007) 1774–1781.
[43] J. Zhang, M. Oyama, Electrochem. Commun. 9 (3) (2007) 459–464.
[44] M.S. El-Deab, T. Somotmura, T. Ohsaka, J. Electrochem. Soc. 152 (1) (2005) C1–C6.
[45] S. Wang, D. Du, Sens. Actuat. B 97 (2004) 373–378.
[46] J. Luo, P.N. Njoki, D. Mott, L. Wang, C.-J. Zhong, Langmuir 22 (2006) 2892–2898.
[47] J. Luo, P.N. Njoki, D. Mott, L. Wang, C.-J. Zhong, Electrochem. Commun. 8 (2006) 581–587.
[48] T. Selvaraju, R. Ramaraj, Electrochem. Commun. 5 (2003) 667–672.
[49] G. Sauerbrey, Z. Phys. 155 (1959) 206–222.
[50] S. Brukenstein, M. Shay, Electrochim. Acta 30 (1985) 1295–1300.
[51] D.V. Ca, L. Sun, J.A. Cox, Electrochim. Acta 51 (2006) 2188–2194.
[52] Y. Liu, M. Yang, Z. Zheng, B. Zhang, Electrochim. Acta 51 (2005) 605–610.
[53] S. Anita, K. Ashavani, C. Moneesha, P. Renu, S. Murali, J. Mater. Chem. 14 (2004) 2696–2702.
[54] M. Saikat, K.A. Sujatha, D. Suguna, Adyanthaya, P. Renu, S. Murali, J. Mater. Chem. 14 (2004) 43–47.
[55] J.E. Huang, D.J. Guo, Y.G. Yao, H.L. Li, J. Electroanal. Chem. 577 (2005) 93–97.
[56] H.F. Cui, J.S. Ye, W.D. Zhang, J. Wang, F.S. Sheu, J. Electroanal. Chem. 577 (2005) 295–302.
[57] V. Radmilovic, H.A. Gasteiger, P.N. Ross, J. Catal. 154 (1995) 98–106.
[58] H. Yao, Y. Sun, X. Lin, Y. Tang, L. Huang, Electrochim. Acta 52 (20) (2007) 6165–6171.
[59] U. Yogeswaran, S.-M. Chen, Electrochim. Acta 52 (19) (2007) 5895–5996.